

3 **Main Manuscript for**

4 **Evidence for microbially-mediated tradeoffs between growth and defense**
5 **throughout coral evolution**

6 Hannah E. Epstein¹, Tanya Brown², Ayomikun O. Akinrinade^{2,3}, Ryan McMinds^{1,4}, F. Joseph
7 Pollock^{5,6}, Dylan Sonett⁷, Styles Smith⁵, David G. Bourne^{8,9}, Carolina S. Carpenter^{10,11}, Rob
8 Knight¹¹⁻¹⁴, Bette L. Willis^{8,15}, Mónica Medina⁵, Joleah B. Lamb³, Rebecca Vega Thurber¹, Jesse
9 R. Zaneveld^{2*}

10 ¹*Department of Microbiology, Oregon State University, 226 Nash Hall, Corvallis, OR 97331, USA*

11 ²*School of Science, Technology, Engineering, and Mathematics, Division of Biological Sciences,
University of Washington Bothell, UWBB-277, Bothell, WA 98011, USA*

13 ³*Department of Ecology and Evolutionary Biology, University of California, Irvine, CA 92697, USA*

14 ⁴*Center for Global Health and Infectious Diseases Research, University of South Florida, 13201 Bruce
15 B. Downs Blvd, MDC 56, Tampa, FL 33612, USA*

16 ⁵*Department of Biology, Pennsylvania State University, 208 Mueller Lab, University Park, PA 16802,
17 USA*

18 ⁶*Hawai‘i & Palmyra Program, The Nature Conservancy, Honolulu, HI, USA*

19 ⁷*School of Pharmacy, University of Washington, Seattle, WA 98195, USA*

20 ⁸*College of Science and Engineering, James Cook University, Townsville, Queensland 4811, Australia*

21 ⁹*Australian Institute of Marine Science, Townsville, Queensland 4810, Australia*

22 ¹⁰*Scripps Institution of Oceanography, University of California, San Diego, La Jolla, CA 92093, USA*

23 ¹¹*Center for Microbiome Innovation, University of California, San Diego, La Jolla, CA 92093, USA*

24 ¹²*Department of Pediatrics, University of California, San Diego, La Jolla, CA 92093, USA*

25 ¹³*Department of Computer Science & Engineering, University of California, San Diego, La Jolla, CA
26 92093, USA*

27 ¹⁴*Micronoma Inc., San Diego, La Jolla, CA 92121, USA*

28 ¹⁵*ARC Centre of Excellence for Coral Reef Studies, James Cook University, Townsville, Queensland
29 4811, Australia*

30

31 *Jesse R. Zaneveld

32 Email: zaneveld@uw.edu

33 **Author Contributions:** The “Global Coral Microbiome Project” was designed and funded by RM,
34 FJP, DGB, BLW, MM, RVT and JRZ. RM, FJP, BLW, MM, JBL, RVT, and JRZ contributed to
35 sample and data collection. RM, FJP, SS, CSC, and RK undertook sample processing and
36 sequencing. Bioinformatic processing and sequence data management was completed by HEE,
37 TB, DS, CSC, RK, and JRZ. Conceptual input for this manuscript was provided by HEE, TB,
38 AOA, RM, JBL, RVT, and JRZ. Statistical analyses and initial draft writing were completed by
39 HEE, TB, AOA, and JRZ. Figures were produced by HEE, TB, and JRZ. All authors contributed to
40 manuscript editing and finalization.

41 **Competing Interest Statement:** The authors declare no competing interests.

42 **Classification:** Major – Biological Sciences; Minor - Microbiology

43 **Keywords:** Evolutionary tradeoffs; Evolution, Coral Disease, Coral Microbiome, Coral Reefs

44 **This PDF file includes:**

45 Main Text

46 Figures 1 to 4

47 **Abstract**

48

49 Evolutionary tradeoffs between life-history strategies are central to animal evolution. However,
50 because microbes can influence aspects of host physiology, behavior, and resistance to stress or
51 disease, changes in animal-microbial symbioses have the potential to mediate life-history
52 tradeoffs. Scleractinian corals provide a highly biodiverse and data-rich host system to test this
53 idea, made more relevant by increases in coral disease outbreaks as a result of anthropogenic
54 changes to climate and reef ecosystems. Identifying factors that determine coral disease
55 susceptibility has therefore become a focus for reef conservation efforts. Using a comparative
56 approach, we tested if coral microbiomes correlate with disease susceptibility across 425 million
57 years of coral evolution by combining a cross-species coral microbiome survey (the “Global Coral
58 Microbiome Project”) with long-term disease prevalence data at multiple sites. Interpreting these
59 data in their phylogenetic context, we show that microbial dominance and composition predict
60 disease susceptibility. We trace this dominance-disease association to a single putatively
61 beneficial bacterial symbiont, *Endozoicomonas*, whose relative abundance in coral tissue
62 explained 30% of variation in disease susceptibility and 60% of variation in microbiome
63 dominance across 40 coral genera. Conversely, *Endozoicomonas* abundances in coral tissue
64 strongly correlated with high growth rates. These results demonstrate that the evolution of
65 microbial symbiosis in corals correlates with both disease prevalence and growth rate.
66 Exploration of the mechanistic basis for these findings will be important for our understanding of
67 how microbial symbiosis influences animal life-history tradeoffs, and in efforts to use microbes to
68 increase coral growth or disease resistance *in-situ*.

69 **Significance Statement**

70

71 The evolution of tropical corals, like that of many organisms, involves tradeoffs in life-history
72 strategy. We sought to test whether microbes influence coral life-history traits. Comparative data
73 from a census of modern coral microbes, combined with long term disease surveys in three
74 regions, provide evidence for a correlation between microbiome structure, growth rate, and
75 disease susceptibility during coral evolution. These trends were driven primarily by changes in
76 the relative abundance of *Endozoicomonas* in coral tissue microbiomes, suggesting the novel
77 hypothesis that *Endozoicomonas* may allow corals to grow more quickly at the cost of greater
78 vulnerability to disease. Thus, symbiosis with microbes may be an important aspect of animal life-
79 history strategy.

80 **Main Text**

81 **Introduction**

82 Tradeoffs in life-history strategy are key features in animal evolution (1, 2). These tradeoffs often
83 involve differential investments in life-history traits such as growth rate (3); reproductive
84 maturation, timing, and fecundity (4); or resistance to stress (5), predation (6) or disease (7). The
85 fitness costs and benefits of these investments are often context-dependent. Thus, shifts in
86 ecological or environmental conditions can favor some life-history strategies over others (5),
87 sculpting trait evolution within animal lineages and reshaping ecological communities. Global
88 climate change is shifting the patterns and prevalence of disease in many animal taxa, while
89 increasing the virulence of some pathogens (8, 9). Identifying evolutionary tradeoffs and resulting
90 trait correlations associated with disease susceptibility (10) can therefore help predict how
91 species survival will shift with climate change.

92 Although much research on evolutionary tradeoffs focuses on the traits of animals themselves, it
93 is also well documented that the physiology (11), fitness and even behavior (12) of many animals
94 are influenced by their microbiomes. Ecological microbiome surveys and laboratory experiments
95 using germ-free animals have linked animal microbiomes, and specific symbionts within them, to
96 multiple key life-history traits, including growth (13), development rate (13), fecundity (13), stress
97 resistance (11, 14), and disease susceptibility (14). It therefore seems likely that microbial
98 symbiosis is an important aspect of animal life-history tradeoffs.

99 If microbes do influence life-history traits (or vice versa), microbiome structure and membership
100 may correlate with those traits over long periods of animal evolution. However, testing the
101 potential relevance of microbial symbiosis for life-history strategy over evolutionary time periods is
102 challenging. These tests must use phylogenetic comparative methods that account for trait
103 correlations induced by the shared history of traits over evolution. They further require large
104 cross-species datasets on both animal traits and microbiome structure. Scleractinian corals meet
105 these data requirements and are therefore an animal lineage that present a unique opportunity to
106 answer the question of whether microbes and life-history strategies are associated.

107 The reef-building corals that have evolved over 425 million years represent a diverse group of
108 animals, including an estimated >1600 species (15), with an extensive fossil record, and a well-
109 known variety in both life-history strategy (2) and microbial symbiosis (16–18). These animals
110 also have special ecological and societal importance, as corals are foundational to reef
111 ecosystems that support some of the most biodiverse assemblages on the planet. These
112 ecosystems in turn support the livelihoods of the many coastal communities that rely on them for
113 food, coastal protection, and recreation (19). Yet the ancient diversity of coral reefs is currently
114 threatened by global climate change, which is driving both dramatic mass bleaching events and
115 increased prevalence and severity of disease outbreaks (8). Due to the threats to coral reef
116 ecosystems, and the potential harm that their collapse could inflict on millions of people in coastal
117 communities worldwide, corals and their microbiomes have been intensively researched.

118 Association with specific dinoflagellate symbionts (e.g., *Durusdinium* vs. *Cladocopium*) has been
119 reported to have complex and species-specific influences on coral traits such as thermal
120 tolerance and growth rate (20) but see (21)). Evolutionary studies have demonstrated that
121 vertical vs. horizontal transmission of these dinoflagellate symbionts is tied to important host
122 traits, such as reproduction by brooding vs. spawning (22). However, potential influences of
123 symbiosis with bacteria and archaea on coral life-history traits are less well understood.

124 Coral microbiome research has demonstrated that in the present-day communities of coral-
125 associated bacteria and archaea (hereafter ‘coral microbiomes’) are influenced by host traits;
126 local environmental factors, such as temperature, depth, nutrient availability, and turbidity;

127 anatomy (16); and ecological context, such as predation, exploitation by farming fish (23), or
128 competition with turf algae. Specific microbes have been shown to protect corals from pathogens
129 through antimicrobial production (24), predation (25), jamming of quorum-sensing systems (26),
130 and passive competition for space and resources. Differences in microbiome structure or
131 dynamics are also often found between related species that show different patterns of disease
132 susceptibility (27). These examples provide support for connections between coral life-history,
133 microbiome structure and disease susceptibility in the present day, although they do not directly
134 allow for statistical testing of evolutionary hypotheses.

135 Clarifying whether microbiome structure and coral life-history traits correlate over coral evolution
136 globally would provide vital context for interpreting studies of extant coral symbiosis and disease
137 at local or regional scales. Several lines of research have created a strong foundation on which
138 such comprehensive comparative evolutionary analyses can be built. Coral disease patterns have
139 been intensively researched, and an increasing number of datasets are now openly available.
140 Well-curated global databases of coral physiological traits (28), with contributions from numerous
141 research groups, have been established and mapped to coral life-history strategies (2). Finally,
142 several large cross-species studies of corals and their microbiomes have been launched. These
143 advances provide an opportunity to compare host trait data and microbiome structure from across
144 the coral tree of life.

145 Here, we test whether microbiome structure correlates with coral disease susceptibility, growth
146 rate, or overall life-history strategy. To address this question quantitatively, we first characterized
147 the microbiome composition from visibly healthy samples of 40 coral genera using 16S rRNA
148 gene sequencing results from the Global Coral Microbiome Project (16)(Supplementary Data
149 Table 1a), and subsequently combined these data with genus-level long-term disease prevalence
150 data from several tropical regions around the globe (the Caribbean (Florida Reef Resilience
151 Project data (FRRP, <https://frrp.org/>), central Pacific (Hawai'i Coral Disease Database
152 (HICORDIS) (29)), and eastern Australia (this study); Supplementary Data Table 1b), and coral
153 life-history traits from the Coral Trait Database (28) (Fig. 1). With the resulting microbiome
154 structure, disease prevalence, and coral growth data across a global distribution of coral genera
155 (Supplementary Data Table 1c), we compared these traits using methods that account for
156 phylogenetic correlations using a time-calibrated multi-gene reference tree of corals (30).

157 Across coral evolution, we found that microbiome structure in healthy corals is correlated with
158 both disease-susceptibility and growth rate. We further identified these correlations as being
159 primarily driven by a single key bacterial genus, *Endozoicomonas*, a common coral symbiont that
160 often forms aggregates within coral tissue (31) and is hypothesized to be a metabolic mutualist.
161 These results provide an important example of long-term correlations between microbiome
162 structure and host traits (disease susceptibility and growth rate), supporting the notion that
163 microbial symbiosis can have important roles in mediating animal life-history tradeoffs.

164 Results and Discussion

165 **Coral microbiomes are dominated by a small number of bacterial taxa.** The microbiome of
166 corals is often dominated by a few highly-abundant taxa that demonstrate species-specificity (17,
167 18), though why these highly-abundant microbial taxa differ across coral diversity is unknown. To
168 test this, we first identified a restricted set of dominant bacterial or archaeal taxa in visibly healthy
169 corals retrieved from mucus, tissue, and skeleton samples of 40 coral genera. ('Dominant taxa'
170 were defined as those that are most abundant on average within all samples from a given portion
171 of coral anatomy in a given coral genus.) Thirty-eight of the coral genera were dominated by the
172 bacterial classes α - or γ -proteobacteria, which are known to include common coral associates
173 (17), with further detailed taxonomic resolution revealing that the number of dominant bacterial
174 and archaeal genera across compartments also remained limited (Fig. 2A; Supplementary Data
175 Table 2). For example, only 17 genera of bacteria or archaea accounted for the dominant

176 microbes in the tissue microbiomes of all 40 coral genera (this number excludes 4 unclassified
177 'genera' that could not be classified to at least the order level). Mucus and skeleton showed
178 similar trends, with only 16 and 25 dominant genera, plus 2 or 4 unclassified genera, respectively.
179 Across coral genera, *Pseudomonas* was most commonly dominant in mucus (31.4% of coral
180 genera), while *Endozoicomonas* was most commonly dominant in tissue (18%) and *Candidatus*
181 *Amoebophilus* (13.5%) was most commonly dominant in skeleton microbiomes. Currently the
182 influences of microbiome structure and dominance of particular microbial taxa on coral physiology
183 are not yet well understood.

184 **Microbiome richness and evenness do not predict disease susceptibility.** To identify how
185 bacterial communities are structured among globally distributed coral taxa, we characterized
186 alpha diversity within the mucus, tissue, and skeleton compartments for each coral genus using
187 several metrics. These included observed features, which measures richness; and the Gini index,
188 which measures evenness. We visualized the evolution of each of these measures of microbiome
189 alpha diversity using ancestral state reconstruction (Figs. S1A, B), then compared them against
190 disease susceptibility using Phylogenetic Generalized Least Squares (PGLS) analysis. While we
191 hypothesized that coral microbiomes high in overall biodiversity might show reduced disease
192 susceptibility — analogous to the ability of more biodiverse ecosystems to resist invasive species
193 (32) — neither microbiome richness nor evenness were significantly correlated with host disease
194 susceptibility in phylogenetic generalized least squares analysis (PGLS richness vs. disease
195 susceptibility: $R^2 = 0.004$, $p = 0.674$, FDR q = 1; PGLS evenness vs. disease susceptibility $R^2 =$
196 0.028 , $p = 0.274$, FDR q = 1; Supplementary Data Table 3a). Some specific cases of coral genera
197 with low microbiome richness and high disease susceptibility were identified (i.e., *Pocillopora*,
198 *Acropora*, and *Montipora*; Figs. S1A, B) but there was no overall trend across all genera surveyed
199 (Fig. 2B). Thus, microbiome richness or evenness alone does not predict coral disease
200 susceptibility.

201 **Microbiome dominance correlates with coral disease susceptibility.** Given that neither
202 microbiome richness nor evenness significantly predicted disease susceptibility, and that cross-
203 species differences in a limited number of dominant microbes were very notable in the data, we
204 hypothesized that corals with highly abundant bacterial taxa might display more disease
205 vulnerability. To quantify this, ecological dominance among identified ASVs was calculated using
206 Simpson's Index, which estimates the probability that two species drawn from a population
207 belong to the same group, and thereby incorporates aspects of both richness and evenness
208 simultaneously. We correlated Simpson's Index against coral disease prevalence for either all
209 coral samples, or those in mucus, tissue, or skeleton considered individually. In coral tissue,
210 microbiome dominance significantly correlated with disease, explaining roughly 27% of overall
211 variation in disease susceptibility across coral species (PGLS: $R^2 = 0.27$, $p = 0.0006$, FDR q =
212 0.025 ; Supplementary Data Table 3a; Fig S1C). No other combination of alpha diversity measure
213 and compartment correlated with disease after accounting for multiple comparisons (Fig. 2B).
214 Thus, microbiome dominance as measured by Simpson's Index was a far stronger predictor of
215 coral disease susceptibility than α -diversity measures that considered either richness or
216 evenness individually.

217 **The association between microbiome dominance and disease strengthens in regionally-**
218 **matched data.** The correlation we saw between microbiome dominance and disease persisted in
219 a regionally-matched comparison between disease and microbiome data, and therefore is
220 unlikely to be driven by biogeographic confounders. While the trend between microbiome
221 dominance and coral disease is compelling across our full dataset, not all coral diseases are
222 cosmopolitan and some exist in only one or a few locations (33). As mismatches between region
223 and disease biogeography could confound our overall results, we sought to assess whether
224 large-scale regional effects drive this trend. For example, perhaps high-dominance corals happen
225 to live in high-disease areas, resulting in incidental correlations between dominance and disease.
226 To test for regional effects, we repeated the PGLS analyses restricting the data to only coral

227 microbiomes from Australia, where sampling was most intensive and for which we have long-term
228 disease datasets best-matched to the microbiome data. In this analysis, ecological dominance in
229 Australian coral tissue microbiomes predicted disease prevalence even more strongly under the
230 lowest AICc model (PGLS: $R^2 = 0.49$, $p = 0.00015$, FDR $q = 0.005$). However, this correlation was
231 strong under all models (Supplementary Data Table 3b). A likely explanation for this stronger
232 result is simply that the disease and microbiome data were drawn from the same region in this
233 analysis, whereas in other cases the available disease and microbiome data were only partially
234 regionally matched. These stronger results in the Australia-only model suggest that microbiomes
235 vary enough geographically that disease and microbiome data from the same location produce
236 the clearest correlations.

237 **Beta diversity explains little variation in disease susceptibility.** Animal microbiomes are often
238 conceived of as having some compositions that are associated with health, and others that are
239 dysbiotic or unhealthy. We sought to test whether this same microbiome beta-diversity framework
240 could predict the extent to which healthy members of different coral taxa are vulnerable to
241 disease. To do so, we correlated coral disease susceptibility against the top three principal
242 coordinate (PC) axes from Weighted and Unweighted UniFrac analyses of microbiome beta-
243 diversity. In contrast to the strong association between microbiome dominance and disease,
244 microbial community composition had less pronounced associations with disease susceptibility.
245 Weighted UniFrac PC axis 3 only nominally significantly correlated with disease susceptibility in
246 all compartments, but this relationship did not remain significant after accounting for multiple
247 comparisons (PGLS: $R^2 = 0.26$, $p = 0.04$, FDR $q = 0.90$; Supplementary Data Table 4).

248 **Microbiome dominance vs. disease correlations are driven by γ -proteobacteria.** Ecological
249 dominance itself seems an unlikely structural property to act as a mechanism of disease
250 resistance. Therefore, we investigated if this high-level summary measure reflected the effects of
251 some specific microbe or set of microbes. For example, disease susceptibility among *Acropora*
252 has been shown to correlate with the abundance of *Rickettsiales* in coral tissues (34, 35).

253 To test how shifts in the dominant class of microbes in coral tissue interacted with the dominance-
254 disease correlation, we repeated our previous correlations twice: once in coral genera that are α -
255 proteobacteria dominated, and once in coral genera that are γ -proteobacteria dominated. Both
256 datasets were visualized with ancestral state reconstruction (Figs. S2A, B). Correlations between
257 microbiome dominance and disease were visually apparent only in reconstructions of the γ -
258 proteobacteria dominated corals, and the dominance-disease correlation was far stronger in γ -
259 proteobacteria dominated corals (PGLS: $R^2 = 0.50$, $p = 0.0001$, FDR $q = 0.003$; Supplementary
260 Data Table 3c), where dominance explained most (50%) of the variation in disease susceptibility.
261 In contrast, α -proteobacteria dominated tissue microbiomes showed no discernable dominance-
262 disease correlations either visually or statistically (PGLS: $R^2 = 0.06$, $p = 0.31$, FDR $q = 0.81$;
263 Supplementary Data Table 3c). This suggested that overall dominance-disease correlations are
264 unlikely to be driven by α -proteobacteria, but may be driven by γ -proteobacteria or specific taxa
265 within this bacterial class. Critically, nothing about these results contradicts the possibility that
266 some α -proteobacteria are coral pathogens, parasites, or opportunists (36). It merely suggests
267 that in healthy corals, dominance by α -proteobacteria does not predict the overall level of disease
268 susceptibility of coral genera, whereas dominance by one or more γ -proteobacteria does.

269 **The coral symbiont *Endozoicomonas* drives dominance-disease correlations.** Bacteria in
270 the genus *Endozoicomonas* are among the most-studied γ -proteobacterial symbionts of corals. In
271 several species *Endozoicomonas* forms prominent aggregates known as CAMAs (coral
272 associated microbial aggregates) in coral tissue (31). In species where *Endozoicomonas* is
273 common, it frequently decreases in relative abundance during coral bleaching or disease (37),
274 suggesting a commensal or mutualistic rather than opportunistic relationship with host health.
275 Further, it has previously been observed that the family Endozoicomonadaceae shows by far the
276 strongest signal of cophylogeny with coral hosts among tested bacterial families in coral tissue

(16). In the present dataset, *Endozoicomonas* was also the single genus that most typically dominated coral tissue microbiomes (18% of coral genera; Fig. 2A). We therefore tested whether the signal of microbiome dominance on disease susceptibility could be explained by the abundances of dominant taxa, and found that across all corals in our dataset, *Endozoicomonas* abundance explained the overwhelming majority of variation in ecological dominance among coral tissue microbiomes (PGLS: R^2 : 0.60, p = 6.2×10^{-10} , FDR q = 2.5×10^{-9} ; Figs. 2C & 3A; Supplementary Data Table 5a). Further, the relative abundance of *Endozoicomonas* in coral tissue alone explained 30% of variance in overall disease susceptibility (PGLS: R^2 = 0.30, p = 0.0002, FDR q = 0.0004; Fig. 3B; Supplementary Data Table 5a), exceeding the signal from ecological dominance. Thus, prior results linking ecological dominance and overall disease susceptibility appear to be largely explained by changes in *Endozoicomonas* relative abundance over coral evolution.

Coral opportunist abundance in healthy corals does not predict genus-wide disease susceptibility. Correlations between *Endozoicomonas* and disease across the coral tree were initially surprising, as *Endozoicomonas* is not thought to be associated with coral pathogenesis. This raised the question of whether the abundance of known or suspected coral pathogens in apparently healthy corals correlates with cross-genus differences in disease susceptibility. The abundance of bacterial groups containing prominent putative bacterial pathogens (such as *Vibrionales*, *Nostocales* or *Rickettsiales*, see (38)) in healthy corals did not show any correlation with disease susceptibility among coral species when tested (Supplementary Data Table 6). Thus, having high abundances of coral opportunists when healthy does not seem to be a hallmark of disease-susceptible corals. This is mostly expected since the abundance of pathogens typically only increases during stress. These observations in healthy corals leave open the question of what about *Endozoicomonas* causes it to be so strongly correlated with coral disease susceptibility.

Testing for other associations between dominant microbes and disease. After testing *Endozoicomonas* - disease associations as a prior hypothesis, we also sought to put these associations in context by testing for correlations with disease in all other dominant microbial genera found in the study (Fig. 2C; Supplementary Data Table 7a). This scan confirmed that *Endozoicomonas* showed far stronger correlations with disease than other microbes in tissue, mucus, and all compartments together. One additional dominant genus in coral skeleton, *Paramaledivibacter* (Phylum Firmicutes/Bacillota), also correlated with disease susceptibility, though this correlation was only nominally significant (PGLS: R^2 = 0.13, p = 0.018, FDR q = 0.282; Fig. 2C).

We also reran this analysis with all zero relative abundance counts excluded (Supplementary Data Table 7b) to assess whether changes in the abundance of dominant microbes, once they were already present, showed the same or different patterns as the overall analysis. The abundance of *Endozoicomonas* overall (PGLS: R^2 = 0.28, p = 0.0005, FDR q = 0.01), in mucus (R^2 = 0.42, p = 0.00008, FDR q = 0.004), or in tissue (R^2 = 0.35, p = 0.0001, FDR q = 0.004) again showed significant associations with disease, while its abundance in skeleton did not (R^2 = 0.04, p = 0.23, FDR q = 0.95). No other lineages showed significant associations with disease after correction for multiple comparisons. Thus, even considering only coral genera that host *Endozoicomonas*, the relative abundance of this microbe correlates with disease susceptibility.

***Endozoicomonas* is associated with high growth rates.** *Endozoicomonas* is linked to metabolic benefits to the coral host (39, 40) and experimental studies have shown that decreases in its abundance is typical with disease (41, 42) or other health stressors such as bleaching (37). This suggests that the striking correlation between *Endozoicomonas* and disease is not due to pathogenesis by *Endozoicomonas*, but instead might arise due to opportunity costs (e.g., in innate immunity, permissiveness to CAMA formation, or symbiosis with defensive microbes within coral tissue). If maintenance of high abundances of *Endozoicomonas* has fitness costs, they may

327 be balanced by metabolic benefits, and we should expect that *Endozoicomonas* would be more
328 abundant in corals with life-history strategies that favor traits such as rapid growth.

329 If symbiosis with *Endozoicomonas* did play a causal role in coral life-history tradeoffs, we
330 hypothesized that we would see a positive correlation between a beneficial coral trait and
331 *Endozoicomonas* that counterbalances the correlation between *Endozoicomonas* and disease.
332 Given that *Endozoicomonas* is thought to be a metabolic mutualist of corals, and it has recently
333 been suggested to facilitate faster coral growth (43), growth rate seemed like a likely candidate
334 for a potential benefit explaining the persistence of coral-*Endozoicomonas* associations.
335 Depending on the mechanism of action, any such *Endozoicomonas* - growth correlations might
336 depend merely on the presence of *Endozoicomonas*, or alternatively on its relative abundance.
337 Using data from the Coral Trait Database (CTDB; (28)) we tested whether *Endozoicomonas*
338 relative abundance was correlated with growth rate in corals where we detected *Endozoicomonas*
339 (i.e., the effect of relative abundance alone) and in all corals (i.e., the combined effect of presence
340 and abundance). In both cases, we limited this analysis to only corals with replicated growth rate
341 data (>= 5 replicates in the CTDB).

342 While the abundance of *Endozoicomonas* was not correlated with growth rate across all coral
343 genera (tissue PGLS: $R^2 = 0.11$, $p = 0.17$, FDR $q = 0.37$; Supplementary Data Table 8a), across
344 coral genera where *Endozoicomonas* was detected ($n = 17$ genera), its relative abundance in
345 tissue was strongly correlated with growth rate (tissue PGLS: $R^2 = 0.31$, $p = 0.024$, FDR $q =$
346 0.024; Supplementary Data Table 8b). These results are consistent with a pattern in which
347 lineage-specific expansions of *Endozoicomonas* within coral microbiomes correlate with or
348 potentially contribute to growth rate. Thus, *Endozoicomonas* may in part explain, or at least
349 correlate with, about a third of known growth rate differences between coral genera. Across the
350 coral genera surveyed in our dataset, initial, low-level symbiosis with *Endozoicomonas* does not
351 correlate with growth rate, but subsequent expansions of the abundance of *Endozoicomonas*
352 within coral microbiomes co-occur with both higher average growth rates and greater disease
353 susceptibility.

354 **Other microbes associated with growth rate.** We sought to contextualize our results on
355 *Endozoicomonas* and growth rate by examining whether other dominant microbes had similar
356 associations with changes in coral growth rate over evolution (Supplementary Data Table 9a, b,
357 Fig. S3). This analysis revealed several other microbes whose relative abundance in corals
358 where they were present (i.e., excluding zero counts) correlated with coral growth rate.
359 Uncultured Rhodospirillales in family Terasakiellaceae (phylum: Proteobacteria) were strongly
360 and positively correlated with growth in all compartments. Conversely, the relative abundance of
361 *Candidatus Nitrosopumilis* (phylum: Thaumarchaeota) overall or in coral tissue was negatively
362 correlated with growth rate. Finally, the relative abundance of *Enhydrobacter* (phylum:
363 Proteobacteria) in coral mucus was positively correlated with growth.

364 As in our prior *Endozoicomonas*-specific analysis, we repeated these tests including zero counts
365 in order to account for both initial establishment and later increases or reductions in abundance
366 (rather than changes in abundance only). The results were similar, except that *Pseudomonas* in
367 mucus and uncultured Myxococcales in skeleton were significantly associated with growth rate,
368 while *Endozoicomonas* and *Enhydrobacter* were not. Thus, associations between host traits and
369 the microbiome may in some cases depend only on presence or absence, while in other cases
370 like *Endozoicomonas* these host-microbiome associations may track expansions or contractions
371 in microbial relative abundance.

372 Overall, these results suggest that while several microbial taxa correlate positively or negatively
373 with coral growth rates, *Endozoicomonas* appears unique in its association with both growth and
374 disease.

375 **Endozoicomonas may mediate growth-defense tradeoffs during coral evolution.** Having
376 seen that *Endozoicomonas* is correlated with both disease susceptibility and growth-rate in
377 corals, we investigated if these correlations were stronger or weaker than the direct correlation
378 between disease and growth rate in our dataset. Across genera with both growth rate and
379 disease prevalence data, growth and disease susceptibility were positively correlated. However,
380 this correlation had only a modest effect size and was not statistically significant. Thus, in this
381 dataset *Endozoicomonas* showed stronger associations with both growth and disease than these
382 factors showed with one another, regardless of whether the analysis was conducted across all
383 coral genera (tissue PGLS: $R^2 = 0.12$, $p = 0.17$, FDR $q = 0.17$; Supplementary Data Table 10a) or
384 just those where *Endozoicomonas* was present (tissue PGLS: $R^2 = 0.06$, $p = 0.37$, FDR $q = 0.37$;
385 Supplementary Data Table 10b). This suggested that *Endozoicomonas* relative abundance might
386 not merely mark tradeoffs between growth and disease but may play some causal role in one or
387 both processes.

388 **Phylogenetic path analysis of growth, disease, and *Endozoicomonas* abundance.** The
389 univariate correlations between *Endozoicomonas*, host disease susceptibility and growth rate
390 raise the question of the direction of causality by which these factors have become non-randomly
391 associated during coral evolution. Using phylogenetic path analysis (Methods), we compared 14
392 models of the relationship between *Endozoicomonas* relative abundance, disease susceptibility,
393 and growth rate (Supplementary Data Table 11a, Fig. S4).

394 As is common in this type of analysis, more than one model was consistent with the data.
395 However, none of the top models using either BM (Supplementary Table 11b) or Pagel's lambda
396 (Supplementary Data Table 11c) suggested that disease influenced growth rate or vice versa
397 without the influence of *Endozoicomonas* (Fig. 3D), and all significant models include
398 *Endozoicomonas*. Thus, while the precise feedback remains to be determined, causality analysis
399 suggests that, in some capacity, *Endozoicomonas* likely mediates growth rate and disease.

400 **Potential mechanisms of action.** The findings of positive correlations between
401 *Endozoicomonas*, host growth rate, and host disease susceptibility documented in this study
402 complement and contextualize much of the ongoing work on the mechanisms underlying
403 proposed coral-*Endozoicomonas* metabolic mutualism (39, 43) and suggest that the interaction of
404 *Endozoicomonas* with coral disease susceptibility deserves greater scrutiny. They also echo
405 findings of correlations between life-history strategy and microbiome structure in other important
406 marine invertebrates, such as that between predator defense and microbial abundance in marine
407 sponges (44).

408 The mechanism by which corals with high proportions of *Endozoicomonas* become more
409 vulnerable to disease are not yet known, but potential explanations fall into three main categories:
410 ecological, structural, or immunological.

411 Many coral microbes (but not *Endozoicomonas*) are thought to protect against pathogenic
412 disease by mechanisms such as antibiotic secretion (24), direct predation (25), jamming of
413 quorum signaling (26), and through physically occupying space close to host tissues that may
414 restrict binding sites for opportunists and pathogens. In theory, it is possible that
415 *Endozoicomonas* abundance may interact with other aspects of coral microbial ecology, thereby
416 reducing microbially-derived host defenses. However, that *Endozoicomonas* are frequently
417 observed in discrete CAMAs complicates this possibility, as any effects on microbes outside the
418 local area of these CAMAs would have to rely on indirect consequences of *Endozoicomonas*-
419 coral interactions or secreted factors. Nevertheless, if this hypothesis were correct, the reductions
420 in the abundance of *Endozoicomonas* that are often reported in diseased coral phenotypes (e.g.,
421 (37)) would then be adaptive on the part of the host, by allowing proportionally greater growth of
422 other, more protective microbes. This hypothesis could be tested by microbial inoculation
423 experiments that increase *Endozoicomonas* abundances prior to or concurrent with disease
424 exposure, with the prediction that this would increase disease severity (although care must be

425 taken to exclude nutritional benefits from corals directly eating the *Endozoicomonas* confounding
426 the results). More systematic studies of whether high abundances of *Endozoicomonas* are
427 exclusively found in visible CAMAs could also speak to the plausibility of this ecological
428 hypothesis, by clarifying the likely routes for interaction between *Endozoicomonas* and other
429 coral-associated microbes.

430 In addition to ecological interactions, the *Endozoicomonas* - disease susceptibility correlation may
431 also arise as a result of host traits that are permissive for the formation of microbial aggregates.
432 As the cellular processes involved in establishing mutualism, commensalism and pathogenesis
433 often overlap, the same host-microbe interactions that allow *Endozoicomonas* and some other
434 microbes like *Simkania* (43) to aggregate within coral tissues may also be more permissive
435 towards invasion by pathogens. So far known coral pathogens have not been reported to be
436 present within CAMAs. However, other structural mechanisms are possible. For example, the
437 density, morphology, or diversity of septate junctions — which form epithelial barriers similar to
438 tight junctions in chordates (45) — might, in theory, influence the ability of both *Endozoicomonas*
439 and pathogenic microbes to enter coral tissues. This idea could be tested by examining cellular
440 morphology, sequence similarity, and/or gene expression of septate junctions and their
441 constituent components in coral species in which CAMAs did or did not form.

442 Finally, it is possible that coral immunological strategies that permit symbiosis with high
443 abundances of *Endozoicomonas* also tend to make corals more vulnerable to pathogens. Coral
444 species vary in immune investment (as measured by immune parameters like melanin
445 abundance, phenoloxidase activity, etc.), and low immune investment has been observed to
446 correlate with disease susceptibility (46). Some theory predicts that the evolution of more
447 permissive immunological strategies is favored by symbionts that provide metabolic benefits to
448 the host (47). In corals specifically, immune repertoires in key gene families such as TIR-domain
449 containing genes vary greatly between species, which has been hypothesized to influence
450 microbiome structure (48). Indeed, in sequenced coral genomes the copy number of some of
451 these, such as IL-1R receptors, appear to correlate with several features of coral microbiomes,
452 including *Endozoicomonas* abundance (49). Thus, symbiosis with *Endozoicomonas* may promote
453 lower immune investment in corals, which in turn increases disease susceptibility. This
454 hypothesis could be tested by comparing the length of coral-*Endozoicomonas* associations, to
455 see whether longer histories of association lead to low immune investment, or by examining
456 selection on innate immune genes in low vs. high *Endozoicomonas* coral lineages (e.g., by dN/dS
457 ratios).

458 A related immunological explanation would occur if *Endozoicomonas* itself achieves high
459 abundances by suppressing aspects of host immunity. Genomic studies of host-associated
460 *Endozoicomonas* identified variation in the proportion of eukaryote-derived genes and domains
461 as a key feature of strain variation, including some domains thought to suppress immunity-
462 induced apoptosis (50). If representatives of those different strains could be cultured, experiments
463 adding exogenous *Endozoicomonas* might clarify whether *Endozoicomonas* strains have any
464 direct effects on coral immunity, and if so whether they differ from strain to strain.

465 **Conclusions.** Animals evolved in a microbial world. The resulting interactions between animal
466 hosts and their associated microbes influence organismal fitness, and the history of these
467 interactions across generations may influence eco-evolutionary patterns. Using evolutionary
468 analyses of coral microbiomes, we provide evidence that symbiosis with *Endozoicomonas* may
469 mediate growth vs. disease resistance (defensive) tradeoffs. While further manipulative studies
470 are necessary to confirm this finding and determine the directionality of the relationship, evidence
471 for this trend across the coral tree of life is compelling.

472 Our comparative approach suggests that *Endozoicomonas*-dominated lineages of corals may
473 grow more quickly under ideal conditions but are more likely to succumb to coral disease.
474 Because much other work has shown that coral disease is exacerbated by global and local

475 stressors such as climate-change driven heat waves or local pollution events (33, 38), this may
476 make *Endozoicomonas*- dominated coral especially vulnerable to environmental change (Fig. 4).

477 If microbial symbiosis does play a causal role in coral life history tradeoffs in the present day, then
478 identifying microbes underlying those tradeoffs may benefit microbiome manipulation for targeted
479 coral conservation and restoration strategies. While the correlation between *Endozoicomonas*
480 and disease in this work was observed at the genus level (primarily because this is the level of
481 taxonomic specificity for most available disease surveys), future work could examine whether
482 similar trends appear between coral sister species or within coral populations. For example,
483 microbial screening (e.g., (51)) could help identify *Endozoicomonas*-dominated coral species or
484 populations that may be more susceptible to disease and drive the conservation and protection of
485 these individuals or their habitats. Identifying these target corals is perhaps most relevant for
486 coral restoration initiatives that include breeding, nursery propagation and out planting, where
487 coral health is monitored closely and predicting disease susceptibility can inform decision-making.
488 Depending on the mechanism underlying the *Endozoicomonas*-disease susceptibility correlations
489 reported here, *Endozoicomonas*-dominated corals may further represent strong candidates for
490 microbiome engineering (e.g., human-assisted manipulation of host-associated microbes (52) or
491 the application of probiotics (14, 53)) to enhance host resilience in anticipation of stress events by
492 decreasing microbiome dominance. That said, we emphasize that microbiome manipulation and
493 other restoration initiatives are not replacements for efforts to decarbonize global economies to
494 limit greenhouse gas emissions.

495 The results presented here provide the first evidence of a likely microbe-mediated life-history
496 tradeoff in scleractinian corals. Further exploration of this and other such potential tradeoffs may
497 shed light on the evolutionary interplay between microbes and the physiology and ecology of their
498 animal hosts.

499 Materials and Methods

500

501 **Coral sample collection and 16S rRNA pre-processing.** 16S rRNA sequence data was
502 obtained from visibly healthy coral DNA extractions collected and processed for the Global Coral
503 Microbiome Project (GCMP). This included coral samples taken from eastern and western
504 Australia that were used in a previous study by Pollock and co-authors (16) in addition to coral
505 samples taken from the Red Sea, Indian Ocean, Coral Triangle, Caribbean, and Eastern Pacific.
506 All samples compared in this study were collected, processed, and sequenced using consistent
507 protocols as outlined below. In total, 1,440 coral, outgroup, and environmental samples were
508 collected. Of these GCMP samples, the 1,283 scleractinian coral and outgroup samples were
509 used in the present study (Supplementary Data Table 1a). These comprise 132 species and 64
510 genera of corals originating from 42 reefs spanning the Pacific, Indian, and Atlantic oceans.

511 The collection and processing of these coral samples followed the methods outlined in Pollock et
512 al (16) and are compatible with samples processed for the Earth Microbiome Project (54). Briefly,
513 three coral compartments were targeted for each sample: tissue, mucus, and skeleton. Mucus
514 was released through agitation of coral surface using a blunt 10mL syringe for approximately 30
515 seconds and collected via suction into a cryogenic vial. Small coral fragments were collected by
516 hammer and chisel or bone shears for both tissue and skeleton samples into sterile WhirlPaks
517 (Nasco Sampling, Madison, WI). All samples were frozen in liquid nitrogen on immediate return to
518 the surface prior to processing. In the laboratory, snap frozen coral fragments were washed with
519 sterile seawater and the tissue was separated from skeleton using sterilized pressurized air at
520 between 800-2000 PSI. Tissue and skeleton samples were then preserved in PowerSoil DNA
521 Isolation kit (MoBio Laboratories, Carlsbad, CA; now Qiagen, Venlo, Netherlands) bead tubes,
522 which contain a guanidinium preservative, and stored at -80°C to await further processing.
523 Outgroup non-scleractinian Anthozoans were also opportunistically collected and stored similarly,
524 including healthy samples of the genera *Millepora* (hydrozoan fire coral), *Palythoa* (zoanthid),
525 *Helioipora* (blue coral), *Tubipora* (organ pipe coral), and *Xenia* and *Lobophytum* (soft corals).

526 Bacterial and archaeal DNA were extracted using the PowerSoil DNA Isolation Kit (MoBio
527 Laboratories, Carlsbad, CA; now Qiagen, Venlo, Netherlands). To select for the 16S rRNA V4
528 gene region, polymerase chain reaction (PCR) was performed using the following primers with
529 illumina adapter sequences (underlined) at the 5' ends: 515F (55) 5'- TCG TCG GCA GCG TCA
530 GAT GTG TAT AAG AGA CAG GTG YCA GCM GCC GCG GTA A -3' and 806R (56) 5'- GTC
531 TCG TGG GCT CGG AGA TGT GTA TAA GAG ACA GGG ACT ACN VGG GTW TCT AAT -3').
532 PCR, library preparation, and sequencing on an Illumina HiSeq (2x125bp) was performed by the
533 EMP (54). All raw sequencing data and associated metadata for the samples used in this study
534 are available on Qiita (qiita.ucsd.edu) under project ID 10895, prep ID 3439.

535 **Sequence assembly, quality control and taxonomic assignment.** 16S rRNA sequencing data
536 were processed in Qiita (57) using the standard EMP workflow. Briefly, sequences were
537 demultiplexed based on 12bp Golay barcodes using “split_libraries” with default parameters in
538 QIIME1.9.1 (58) and trimmed to 100bp to remove low quality base pairs. Quality control (e.g.,
539 denoising, de-replication and chimera filtering) and identification of amplicon sequence variants
540 (ASVs) were performed on forward reads using deblur 1.1.0 (59) with default parameters. The
541 resulting biom and taxonomy tables were obtained from Qiita (CRC32 id: 8817b8b8 and CRC32
542 id: ac925c85) and processed using a customized QIIME2 v. 2020.8.0 (60) pipeline in python
543 (github.com/zaneveld/GCMP_global_disease). Taxonomic assignment of ASVs was performed
544 using vsearch (61) with SILVA v. 138 (62).

545 **Removal of cryptic mitochondrial reads.** Coral mitochondrial reads obtained from metaxa2
546 (63) were added to the SILVA repository to better identify host mitochondrial reads that may be
547 present in the sequencing data (64). We refer to this expanded taxonomy as “silva_metaxa2” in
548 code. After taxonomic assignment, all mitochondrial and chloroplast reads were removed. The
549 bacterial phylogenetic tree was built using the SATé-enabled phylogenetic placement (SEPP)
550 insertion technique with the q2-fragment-insertion plugin (65) to account for the short-read
551 sequencing data, again using the SILVA v. 138 (62) database as reference taxonomy. The final
552 output from this pipeline consisted of a taxonomy table, ASV feature table and phylogenetic tree
553 that were used for downstream analyses.

554 **Identification of potential contaminants.** Potential contaminants from extraction and sequence
555 blanks (n = 103 negative controls) were identified and removed using the decontam package (66)
556 in R v. 4.0.2 (67) with a conservative threshold value of 0.5 to ensure all ASVs that were more
557 prevalent in negative controls than samples were removed (n = 662 potential contaminants). The
558 final feature table consisted of a total of 1,383 samples, 195,684 ASVs, and 37,469,008 reads.

559 **Summary of disease data by coral genus.** Disease data were gathered from long-term multi-
560 species surveys in the Florida Keys (the Florida Reef Resilience Program (FRRP),
561 <https://frrp.org/>), Hawai'i (HICORDIS (29)), and Australia (this study). Disease counts for
562 Australian corals were collected over a period of 5 years (2009-2013) across 109 reef sites and
563 65 coral genera (Supplementary Data Table 1b). At each of the 109 reefs, we surveyed coral
564 health using 3 replicate belt transects laid along reef contours at 3-4m depth and approximately
565 20m apart using globally standardized protocols (68). Depending on the reef location, belt
566 transects were either 10, 15, or 20m in length by 2m width making the area surveyed at each reef
567 between 60 and 120m². Within each belt transect, we identified each coral colony over 5 cm in
568 diameter to genus and classified it as either healthy (no observable disease lesions) or affected
569 by one or more of six common Indo-Pacific coral diseases (according to (69)). Together with the
570 FRRP and HICORDIS data, the combined disease dataset contained 582,342 coral observations
571 across 99 coral genera (Supplementary Data Table 1c).

572 Because many of these disease observations identified corals only to genus, disease prevalence
573 data were summarized at the genus level. All three resources represent coral surveys over time,
574 ranging from 5 to 16 years. We chose such long-term datasets in an attempt to minimize the
575 potential effects of specific events (e.g., bleaching in a single summer) and instead to capture

576 more general trends in disease susceptibility across species, if such trends were present.
577 Summarizing these data at the genus level was thus part of a comparative strategy, enabling us
578 to extract overall trends and average out local circumstances, so that we could find holobiont
579 features that control disease resistance that may protect some corals but not others. When
580 summarizing at the genus level, individual counts of healthy corals or corals with specific
581 diseases were summed within coral genera across these datasets.

582 To ensure sufficient replication, we excluded coral genera with fewer than 100 observed
583 individuals. This minimal count was selected because it is the lowest frequency at which diseases
584 with a reasonably high frequency (e.g., 5%) can be reliably detected. (With 100 counts, there is a
585 >95% chance of detecting at least one count of any disease present with $\geq 5\%$ prevalence;
586 cumulative binomial, 100 trials, success chance = 0.05). Because only very rarely observed taxa
587 were removed, this filtering preserved 99.8% of total observations. Ultimately, our genus-level
588 summary produced a table with 581,311 observations across 60 coral genera (Supplementary
589 Data Table 1d).

590 **Summary of the microbiome data by coral host genus.** Statistical summaries of microbiome
591 community composition were calculated for each sample in QIIME2 (60), and then summarized
592 within anatomical compartments and coral genera. These summaries of coral microbiome alpha
593 diversity were richness (observed features per 1000 reads), evenness (the Gini Index), and
594 Simpson's Index, which combines both richness and evenness. Thus, each combination of coral
595 genus and anatomical compartment — such as *Acropora* mucus — was assigned an average α -
596 diversity value.

597 Simpson's Index, which is of particular importance in these results, is at its highest when a single
598 taxon is the only one present in microbiome, and at its lowest when there are both a large number
599 of taxa, and all taxa have equal abundance. Thus, this measure is reduced both by community
600 richness and community evenness (Simpson's Index is closely related to Simpson's Diversity,
601 which is calculated as 1 - Simpson's Index, such that more rich or even communities produce
602 higher values).

603 **Construction of a genus level trait table.** The summarized, genus-level disease susceptibility
604 data compiled from all disease projects, and the summarized genus-level microbiome diversity
605 data (see above) were combined to form a trait table that was used in subsequent evolutionary
606 modeling. Additionally, the relative abundance of 'dominant' microbes analyzed in this study was
607 averaged within genera and added to this genus-level trait table.

608 **Genus-level summary of a reference coral phylogeny.** Starting with a previously published
609 multigene time-calibrated phylogeny of corals (30) that we had previously used to demonstrate
610 phyllosymbiosis in corals (16), we randomly selected one representative species per genus to
611 produce a genus level tree. This approach was preferred over several alternatives — such as
612 trimming the tree back to the last common ancestor of each genus and reconstructing trait values
613 — because it required fewer assumptions about the process of trait evolution. As microbiome
614 data were not available for all genera on the coral tree (e.g., temperate deep sea corals), the tree
615 was further pruned to include only the subset of branches that matched those with microbiome
616 data.

617 **Addition of genus-level coral growth data.** To examine the influence of microbiome structure
618 on coral traits, we pulled growth data from the Coral Trait Database (28) from all coral genera that
619 matched those with both microbiome and disease data, and were collected using consistent
620 metrics (mm/yr). This resulted in growth rate data from 18 coral genera that were subsequently
621 combined with our genus-level trait table (Supplementary Data Table 1d).

622 **Phylogenetic Correlative Analysis.** Shared evolutionary history induces correlations in traits
623 between species that violate the requirement of standard statistical tests that observations must

624 be independent and uncorrelated. Thus, special care must be taken to account for phylogeny in
625 comparative analysis. We first applied Felsenstein's phylogenetic independent contrasts (PIC) to
626 visualize our cross-genus trait correlations using the phytools R package (70). This method
627 removes the effect of any shared evolutionary histories by calculating differences in trait values
628 (contrasts) between sister taxa. We next examined the relationships between traits using
629 information-theoretic model selection (that is, comparison of AICc scores) to identify phylogenetic
630 generalized least squares (PGLS) models of evolution that best explained the observed
631 distribution of microbiome α - or β -diversity and disease susceptibility (as continuous evolutionary
632 characters) in extant species. We tested 4 evolutionary models in the caper R package (71). In
633 the first model, we used PGLS with no branch length transformation (i.e. holding $\lambda, \delta, \kappa = 1$). Thus,
634 this first model is equivalent to PIC. In the next 3 models, we transformed branch lengths on the
635 tree by allowing the model to fit either λ , δ , or κ (see below) using maximum likelihood estimation,
636 while fixing the other 2 parameters at 1. We refer to these 4 models as PGLS, PGLS + λ , PGLS +
637 δ , and PGLS + κ . For detailed explanations of each parameter, please refer to Supplementary
638 Data Table 12. Typically, these models estimated very low λ (~ 0), indicating little or low
639 phylogenetic inertia. R^2 and p -values were adjusted for multiple comparisons using a false
640 discovery rate (FDR) correction. Significant relationships between the two traits suggests that
641 they are evolutionarily correlated. Data were visualized by plotting phylogenetic contrasts and all
642 statistics reported represent the best PGLS model results.

643 Additionally, ancestral state reconstructions of key traits were visualized using the contmap
644 function in the phytools R package (70), which in turn estimates internal states using fast
645 maximum-likelihood (ML) ancestral state reconstruct as implemented in the fastAnc phytools
646 function.

647 **Phylogenetic causality analysis.** Observing that A and B are correlated famously does not
648 guarantee that A causes B. However, non-random correlation between A and B does imply some
649 causal association - though there are many possibilities (A causes B, B causes A, a positive
650 feedback loop exists between A & B, some external factor C causes both A and B, etc.). Path
651 analysis represents hypotheses of causality using directed acyclic graphs, then tests the different
652 strengths of association predicted under different hypotheses of causation to test which are
653 consistent with data. The cross-species nature of these data further necessitated use of
654 phylogenetic path analysis, which also accounts for expected trait correlations among related
655 genera. Hypotheses of the direction of causality between microbiome (specifically
656 *Endozoicomonas*), disease, and growth rate were tested using a phylogenetic causality analysis
657 performed in the R package phylopath (72). This analysis tests the ability of different models to
658 explain correlations in trait data. For example, does selection for a high growth rate in turn drive
659 selection for increased *Endozoicomonas* abundance, which then increases disease susceptibility,
660 or does symbiosis with *Endozoicomonas* itself separately increase disease and growth? Fourteen
661 potential causality models were tested to incorporate all biologically plausible pathways between
662 *Endozoicomonas* abundance, disease susceptibility, and growth rate (Supplementary Data Table
663 11a; Fig. S4). The top performing causality models according to CICc values (using both Pagel's
664 λ and Brownian Motion models of evolution) were averaged for interpretation and visualization.

665 Acknowledgments

666 The authors would like to acknowledge many contributors for their field assistance during
667 collection of Global Coral Microbiome Project data in this manuscript. These include: Tasman
668 Douglass, Margaux Hein, Frazer McGregor, Kathy Morrow, Katia Nicolet, Cathie Page, and
669 Gergely Torda for their field assistance in Australia; Valeria Pizarro, Mateo López-Victoria, Alaina
670 Weinheimer, Claudia Tatiana Galindo Martínez for Assistance in Colombia; Chris Voolstra, Maren
671 Ziegler, Anna Roik, and many others at King Abdullah University of Science and Technology
672 (KAUST) for field assistance in Saudi Arabia; Mark Vermeij, Kristen Marhaver, Pedro Frade, Ben
673 Mueller, and others at CARMABI for field assistance during sampling in Curaçao; Danwei Huang
674

675 for field assistance in Singapore; Ruth Gates, Katie Barrott, Courtney Couch, and Keoki Stender
676 for field assistance in Hawai'i; and Lyndsy Gazda, Jamie Lee Proffitt, Gabriele Swain, and Alaina
677 Weinheimer for their assistance in the laboratory. The authors also acknowledge the staff of the
678 Coral Bay Research Station, Lizard Island Research Station, Lord Howe Island Marine Park, Lord
679 Howe Island Research Station, the Australian Institute of Marine Science, and RV Cape
680 Ferguson for their logistical support. This work was supported by a National Science Foundation
681 Dimensions of Biodiversity grant (#1442306) to RVT and MM, an in-kind UC San Diego Seed
682 Grant in Microbiome Science grant to JZ, an NSF IoS CAREER grant (#1942647) to JZ, and an
683 NSF Postdoctoral Research Fellowship in Biology (#2006244) to HEE.

684 **References**

- 686 1. K. Healy, T. H. G. Ezard, O. R. Jones, R. Salguero-Gómez, Y. M. Buckley, Animal life
687 history is shaped by the pace of life and the distribution of age-specific mortality and
688 reproduction. *Nat. Ecol. Evol.* 3, 1217–1224 (2019).
- 689 2. E. S. Darling, L. Alvarez-Filip, T. A. Oliver, T. R. McClanahan, I. M. Côté, Evaluating life-
690 history strategies of reef corals from species traits. *Ecol. Lett.* 15, 1378–1386 (2012).
- 691 3. P. J. van der Most, B. de Jong, H. K. Parmentier, S. Verhulst, Trade-off between growth
692 and immune function: a meta-analysis of selection experiments. *Funct. Ecol.* 25, 74–80
693 (2011).
- 694 4. A. V. Badyaev, C. K. Ghalambor, Evolution of life histories along elevational gradients:
695 Trade-off between parental care and fecundity. *Ecology* 82, 2948–2960 (2001).
- 696 5. S. S. Padda, J. R. Glass, Z. R. Stahlschmidt, When it's hot and dry: life-history strategy
697 influences the effects of heat waves and water limitation. *J. Exp. Biol.* 224, jeb236398
698 (2021).
- 699 6. R. Tollrian, Predator-induced morphological defenses: costs, life history shifts, and maternal
700 effects in *Daphnia pulex*. *Ecology* 76, 1691–1705 (1995).
- 701 7. R. L. Loehliller, C. Deerenberg, Trade-offs in evolutionary immunology: just what is the
702 cost of immunity? *Oikos* 88, 87–98 (2000).
- 703 8. J. Maynard, *et al.*, Projections of climate conditions that increase coral disease susceptibility
704 and pathogen abundance and virulence. *Nat. Clim. Change* 5, 688–694 (2015).
- 705 9. C. Mora, *et al.*, Over half of known human pathogenic diseases can be aggravated by
706 climate change. *Nat. Clim. Change* 12, 869–875 (2022).
- 707 10. B. J. Parker, S. M. Baribeau, A. M. Laughton, L. H. Griffin, N. M. Gerardo, Life-history
708 strategy determines constraints on immune function. *J. Anim. Ecol.* 86, 473–483 (2017).
- 709 11. L. Baldassarre, H. Ying, A. M. Reitzel, S. Franzenburg, S. Fraune, Microbiota mediated
710 plasticity promotes thermal adaptation in the sea anemone *Nematostella vectensis*. *Nat.*
711 *Commun.* 13, 3804 (2022).
- 712 12. V. O. Ezenwa, N. M. Gerardo, D. W. Inouye, M. Medina, J. B. Xavier, Animal behavior and
713 the microbiome. *Science* 338, 198–199 (2012).
- 714 13. A. W. Walters, *et al.*, The microbiota influences the *Drosophila melanogaster* life history
715 strategy. *Mol. Ecol.* 29, 639–653 (2020).
- 716 14. P. M. Rosado, *et al.*, Marine probiotics: increasing coral resistance to bleaching through

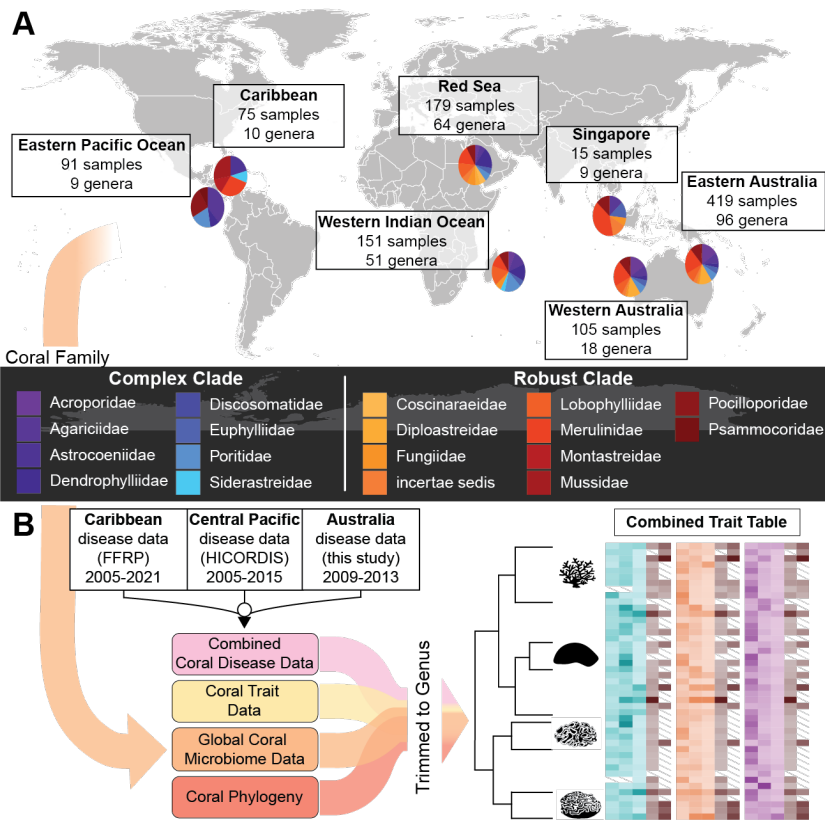
- 717 microbiome manipulation. *ISME J.* 13, 921–936 (2019).
- 718 15. B. W. Hoeksema, Cairns, S., World list of Scleractinia (October 31, 2022).
- 719 16. F. J. Pollock, *et al.*, Coral-associated bacteria demonstrate phylosymbiosis and
720 cophylogeny. *Nat. Commun.* 9, 1–13 (2018).
- 721 17. M. J. Huggett, A. Apprill, Coral microbiome database: Integration of sequences reveals high
722 diversity and relatedness of coral-associated microbes. *Environ. Microbiol. Rep.* 11, 372–
723 385 (2019).
- 724 18. C. M. Dunphy, T. C. Gouhier, N. D. Chu, S. V. Vollmer, Structure and stability of the coral
725 microbiome in space and time. *Sci. Rep.* 9, 6785 (2019).
- 726 19. F. Moberg, C. Folke, Ecological goods and services of coral reef ecosystems. *Ecol. Econ.*
727 29, 215–233 (1999).
- 728 20. R. Berkelmans, M. J. H. van Oppen, The role of zooxanthellae in the thermal tolerance of
729 corals: A 'nugget of hope' for coral reefs in an era of climate change. *Proc. R. Soc. B Biol.*
730 *Sci.* 273, 2305–2312 (2006).
- 731 21. R. N. Silverstein, R. Cunning, A. C. Baker, Tenacious D: *Symbiodinium* in clade D remain in
732 reef corals at both high and low temperature extremes despite impairment. *J. Exp. Biol.*
733 220, 1192–1196 (2017).
- 734 22. A. C. Hartmann, A. H. Baird, N. Knowlton, D. Huang, The paradox of environmental
735 symbiont acquisition in obligate mutualisms. *Curr. Biol.* 27, 3711-3716.e3 (2017).
- 736 23. J. M. Casey, T. D. Ainsworth, J. H. Choat, S. R. Connolly, Farming behaviour of reef fishes
737 increases the prevalence of coral disease associated microbes and black band disease.
738 *Proc. R. Soc. B Biol. Sci.* 281, 20141032 (2014).
- 739 24. J. A. J. M. van de Water, *et al.*, Antimicrobial and stress responses to increased
740 temperature and bacterial pathogen challenge in the holobiont of a reef-building coral. *Mol.*
741 *Ecol.* 27, 1065–1080.
- 742 25. R. M. Welsh, *et al.*, Bacterial predation in a marine host-associated microbiome. *ISME J.*
743 10, 1540–1544 (2016).
- 744 26. J. Li, W. Kuang, L. Long, S. Zhang, Production of quorum-sensing signals by bacteria in the
745 coral mucus layer. *Coral Reefs* 36, 1235–1241 (2017).
- 746 27. S. M. Rosales, *et al.*, Microbiome differences in disease-resistant vs. susceptible *Acropora*
747 corals subjected to disease challenge assays. *Sci. Rep.* 9, 18279 (2019).
- 748 28. J. S. Madin, *et al.*, The Coral Trait Database, a curated database of trait information for
749 coral species from the global oceans. *Sci. Data* 3, sdata201617 (2016).
- 750 29. J. M. Caldwell, *et al.*, Hawai'i Coral Disease database (HICORDIS): species-specific coral
751 health data from across the Hawaiian archipelago. *Data Brief* 8, 1054–1058 (2016).
- 752 30. D. Huang, K. Roy, The future of evolutionary diversity in reef corals. *Philos. Trans. R. Soc.*
753 *B Biol. Sci.* 370, 20140010 (2015).
- 754 31. N. Wada, *et al.*, Characterization of coral-associated microbial aggregates (CAMAs) within
755 tissues of the coral *Acropora hyacinthus*. *Sci. Rep.* 9, 14662 (2019).

- 756 32. J. J. Stachowicz, R. B. Whitlatch, R. W. Osman, Species diversity and invasion resistance
757 in a marine ecosystem. *Science* 286, 1577–1579 (1999).
- 758 33. J. Morais, A. P. L. R. Cardoso, B. A. Santos, A global synthesis of the current knowledge on
759 the taxonomic and geographic distribution of major coral diseases. *Environ. Adv.* 8, 100231
760 (2022).
- 761 34. G. Klings, R. L. Maher, R. L. Vega Thurber, E. M. Muller, Parasitic ‘*Candidatus*
762 *Aquarickettsia rohweri*’ is a marker of disease susceptibility in *Acropora cervicornis* but is
763 lost during thermal stress. *Environ. Microbiol.* 22, 5341–5355 (2020).
- 764 35. L. J. Baker, *et al.*, The coral symbiont *Candidatus Aquarickettsia* is variably abundant in
765 threatened Caribbean acroporids and transmitted horizontally. *ISME J.* 16, 400–411 (2022).
- 766 36. O. Pantos, *et al.*, The bacterial ecology of a plague-like disease affecting the Caribbean
767 coral *Montastrea annularis*. *Environ. Microbiol.* 5, 370–382 (2003).
- 768 37. D. Bourne, Y. Iida, S. Uthicke, C. Smith-Keune, Changes in coral-associated microbial
769 communities during a bleaching event. *ISME J.* 2, 350–363 (2008).
- 770 38. R. Vega Thurber, *et al.*, Deciphering coral disease dynamics: Integrating host, microbiome,
771 and the changing environment. *Front. Ecol. Evol.* 8 (2020).
- 772 39. M. J. Neave, C. T. Michell, A. Apprill, C. R. Voolstra, *Endozoicomonas* genomes reveal
773 functional adaptation and plasticity in bacterial strains symbiotically associated with diverse
774 marine hosts. *Sci. Rep.* 7, 40579 (2017).
- 775 40. K. Tandon, *et al.*, Comparative genomics: Dominant coral-bacterium *Endozoicomonas*
776 *acroporae* metabolizes dimethylsulfoniopropionate (DMSP). *ISME J.* 14, 1290–1303 (2020).
- 777 41. S. Gignoux-Wolfsohn, S. V. Vollmer, F. M. Aronson, Complex interactions between
778 potentially pathogenic, opportunistic, and resident bacteria emerge during infection on a
779 reef-building coral. *FEMS Microbiol. Ecol.* 93, fix080 (2017).
- 780 42. J. L. Meyer, V. J. Paul, M. Teplitski, Community shifts in the surface microbiomes of the
781 coral *Porites astreoides* with unusual lesions. *PLOS ONE* 9, e100316 (2014).
- 782 43. N. Wada, *et al.*, High-resolution spatial and genomic characterization of coral-associated
783 microbial aggregates in the coral *Stylophora pistillata*. *Sci. Adv.* 8, eab02431 (2022).
- 784 44. M. Sabrina Pankey, *et al.*, Cophylogeny and convergence shape holobiont evolution in
785 sponge–microbe symbioses. *Nat. Ecol. Evol.* 6, 750–762 (2022).
- 786 45. P. Ganot, *et al.*, Structural molecular components of septate junctions in cnidarians point to
787 the origin of epithelial junctions in eukaryotes. *Mol. Biol. Evol.* 32, 44–62 (2015).
- 788 46. C. V. Palmer, J. C. Bythell, B. L. Willis, Levels of immunity parameters underpin bleaching
789 and disease susceptibility of reef corals. *FASEB J. Off. Publ. Fed. Am. Soc. Exp. Biol.* 24,
790 1935–1946 (2010).
- 791 47. C. J. E. Metcalf, B. Koskella, Protective microbiomes can limit the evolution of host
792 pathogen defense. *Evol. Lett.* 3, 534–543 (2019).
- 793 48. A. Z. Poole, V. M. Weis, TIR-domain-containing protein repertoire of nine anthozoan
794 species reveals coral-specific expansions and uncharacterized proteins. *Dev. Comp.
795 Immunol.* 46, 480–488 (2014).

- 796 49. T. Brown, *et al.*, Anatomically-specific coupling between innate immune gene repertoire and
797 microbiome structure during coral evolution. *bioRxiv* 2023.04.26.538298 (2023).
798 <https://doi.org/10.1101/2023.04.26.538298> (accessed 1 May 2023).
- 799 50. K. Ide, *et al.*, Targeted single-cell genomics reveals novel host adaptation strategies of the
800 symbiotic bacteria *Endozoicomonas* in *Acropora tenuis* coral. *Microbiome* 10, 220 (2022).
- 801 51. B. Glasl, N. S. Webster, D. G. Bourne, Microbial indicators as a diagnostic tool for
802 assessing water quality and climate stress in coral reef ecosystems. *Mar. Biol.* 164, 1–18
803 (2017).
- 804 52. H. E. Epstein, H. A. Smith, G. Torda, M. J. Oppen, Microbiome engineering: enhancing
805 climate resilience in corals. *Front. Ecol. Environ.* 17, 100–108 (2019).
- 806 53. L. Reshef, O. Koren, Y. Loya, I. Zilber-Rosenberg, E. Rosenberg, The Coral Probiotic
807 Hypothesis. *Environ. Microbiol.* 8, 2068–2073 (2006).
- 808 54. The Earth Microbiome Project Consortium, *et al.*, A communal catalogue reveals Earth's
809 multiscale microbial diversity. *Nature* 551, 457–463 (2017).
- 810 55. A. E. Parada, D. M. Needham, J. A. Fuhrman, Every base matters: assessing small subunit
811 rRNA primers for marine microbiomes with mock communities, time series and global field
812 samples. *Environ. Microbiol.* 18, 1403–1414 (2016).
- 813 56. A. Apprill, S. McNally, R. Parsons, L. Weber, Minor revision to V4 region SSU rRNA 806R
814 gene primer greatly increases detection of SAR11 bacterioplankton. *Aquat. Microb. Ecol.*
815 75, 129–137 (2015).
- 816 57. A. Gonzalez, *et al.*, Qiita: rapid, web-enabled microbiome meta-analysis. *Nat. Methods* 15,
817 796–798 (2018).
- 818 58. J. G. Caporaso, *et al.*, QIIME allows analysis of high-throughput community sequencing
819 data. *Nat. Methods* 7, 335–336 (2010).
- 820 59. A. Amir, *et al.*, Deblur rapidly resolves single-nucleotide community sequence patterns.
821 *mSystems* 2, e00191-16 (2017).
- 822 60. E. Bolyen, *et al.*, QIIME 2: Reproducible, interactive, scalable, and extensible microbiome
823 data science. *Nature Biotechnol.* 37, 852–857 (2019).
- 824 61. T. Rognes, T. Flouri, B. Nichols, C. Quince, F. Mahé, VSEARCH: a versatile open source
825 tool for metagenomics. *PeerJ* 4, e2584 (2016).
- 826 62. C. Quast, *et al.*, The SILVA ribosomal RNA gene database project: improved data
827 processing and web-based tools. *Nucleic Acids Res.* 41, D590–D596 (2013).
- 828 63. J. Bengtsson-Palme, *et al.*, METAXA2: improved identification and taxonomic classification
829 of small and large subunit rRNA in metagenomic data. *Mol. Ecol. Resour.* 15, 1403–1414
830 (2015).
- 831 64. D. Sonett, T. Brown, J. Bengtsson-Palme, J. L. Padilla-Gamiño, J. R. Zaneveld, The
832 organelle in the room: Under-annotated mitochondrial reads bias coral microbiome analysis,
833 *bioRxiv* 2021.02.23.431501 (2021). <https://doi.org/10.1101/2021.02.23.431501> (accessed
834 11 July 2022).
- 835 65. S. Janssen, *et al.*, Phylogenetic Placement of Exact Amplicon Sequences Improves

- 836 Associations with Clinical Information. *mSystems* 3 (2018).
- 837 66. N. M. Davis, D. Proctor, S. P. Holmes, D.A. Relman, B.J. Callahan, Simple statistical
838 identification and removal of contaminant sequences in marker-gene and metagenomics
839 data. *Microbiome* 6, 226 (2018).
- 840 67. R Core Team, R: A language and environment for statistical computing (2021).
- 841 68. L. Raymundo, T. M. Work, A. W. Bruckner, B. Willis, A coral disease handbook: Guidelines
842 for assessment, monitoring, and management (Coral Reef Targeted Research and
843 Capacity Building for Management Program, 2008), pp. 17-32.
- 844 69. J. B. Lamb, *et al.*, Plastic waste associated with disease on coral reefs. *Science* 359, 460–
845 462 (2018).
- 846 70. Revell, Liam J., phytools: An R package for phylogenetic comparative biology (and other
847 things). *Methods Ecol. Evol.* 3, 217–223 (2012).
- 848 71. David Orme, *et al.*, caper: Comparative Analyses of Phylogenetics and Evolution in R
849 (2018).
- 850 72. W. van der Bijl, phylopath: Easy phylogenetic path analysis in R. *PeerJ* 6, e4718 (2018).

851 **Figures and Tables**
 852



853
 854 **Figure 1. Conceptual overview of data sources integrated for the project. A.** Map of
 855 sampling locations for coral microbiomes analyzed in the manuscript. Pie charts show the
 856 proportion of coral samples from families in the Complex clade (cool colors) and Robust clade
 857 (warm colors). Samples were collected from coral mucus, tissue, and endolithic skeleton (see
 858 Methods). **B.** Schematic representation of data integration for the project. Coral microbiome data
 859 (as shown in A) were combined with long-term disease prevalence data from 3 projects (the
 860 Florida Reef Resilience Program (FFRP), the Hawai'i Coral Disease Database (HICORDIS), and
 861 data from Australia (this study)), as well as coral trait data from the Coral Trait Database, and a
 862 molecular phylogeny of corals (see Methods). To integrate data from these disparate sources, all
 863 annotations were pooled at the genus level. The end product was a trait table of microbiome,
 864 taxonomic, physiological, and disease data across diverse coral genera.

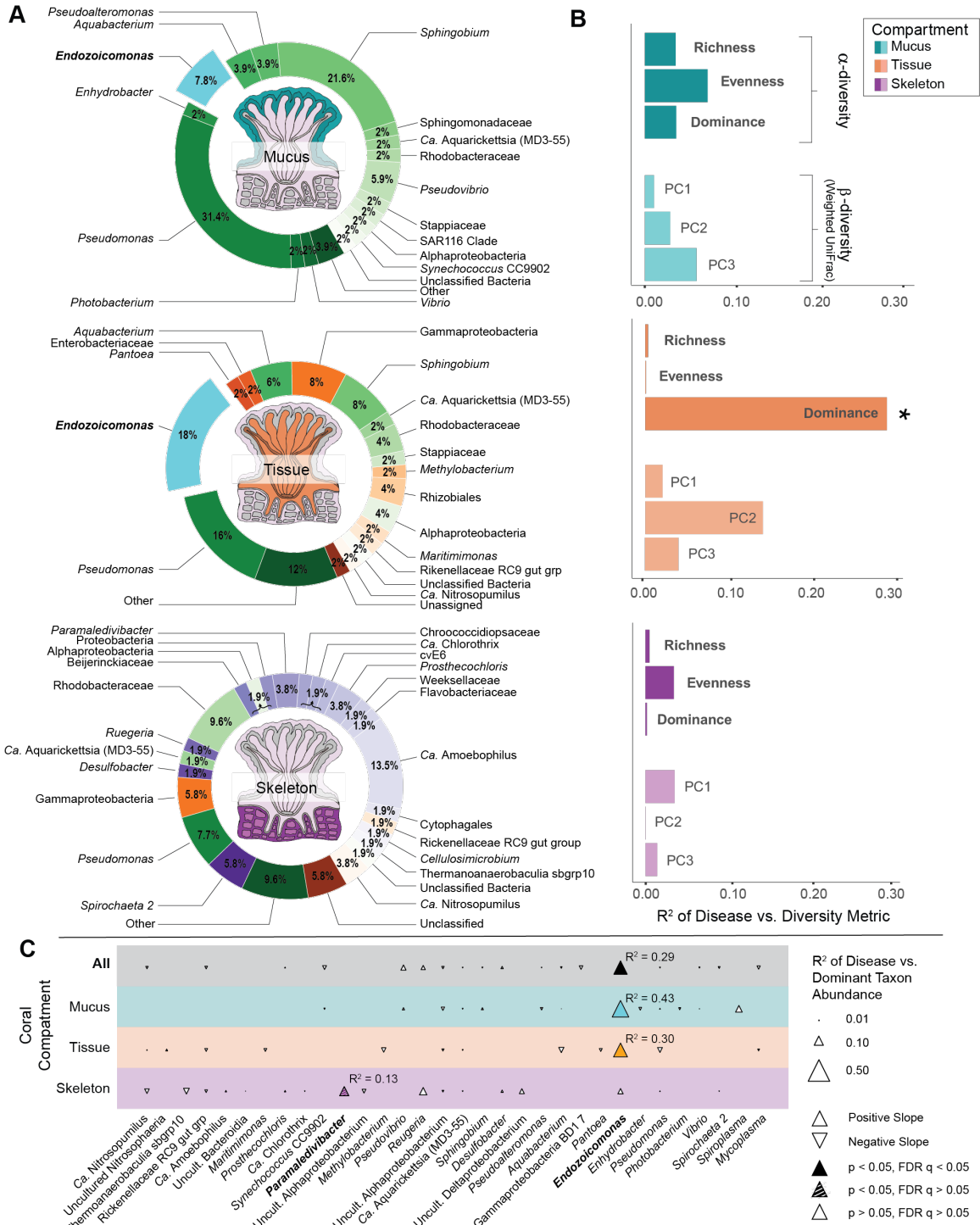
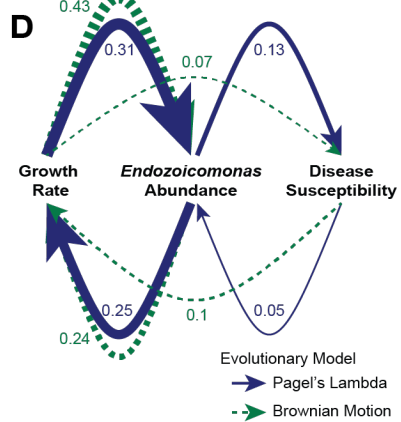
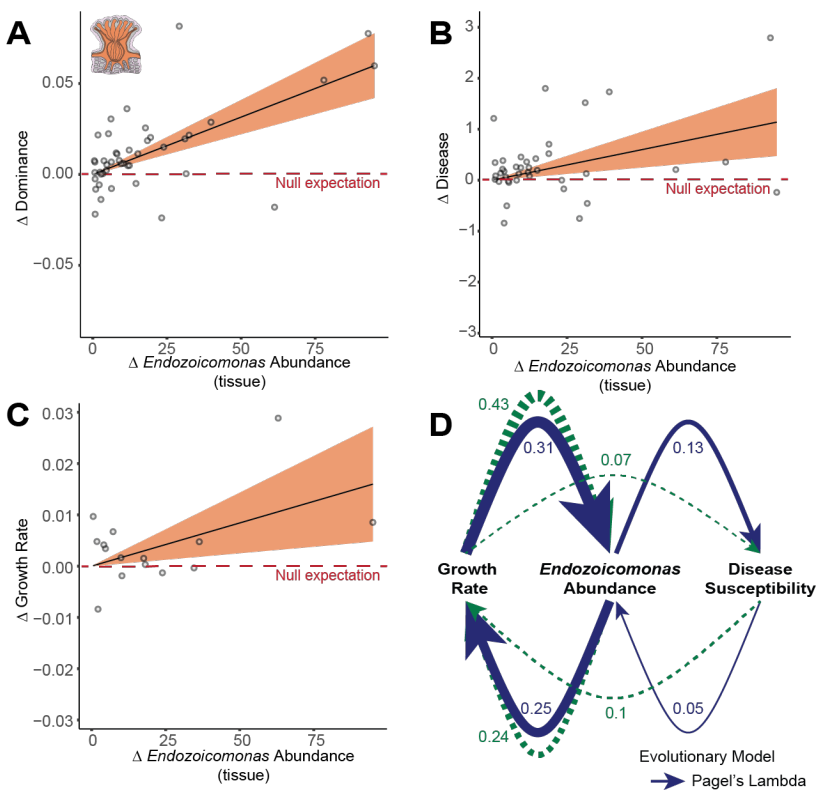


Figure 2. Dominant microbes in the coral microbiome. **A.** Dominant bacterial or archaeal genera in coral mucus (cyan), tissue (orange), or skeleton (purple) microbiomes. Pie wedges represent the fraction of coral host genera in which the labeled bacterium is more abundant than all other bacterial or archaeal taxa. Cyan shades represent microbes dominant in mucus, oranges represent microbes dominant in tissue (but not mucus), purple shades represent microbes dominant in skeleton (but not mucus or tissue). *Endozoicomonas*, which is of special significance later in the paper, is highlighted in aqua. **B.** Bar charts showing correlations between microbiome

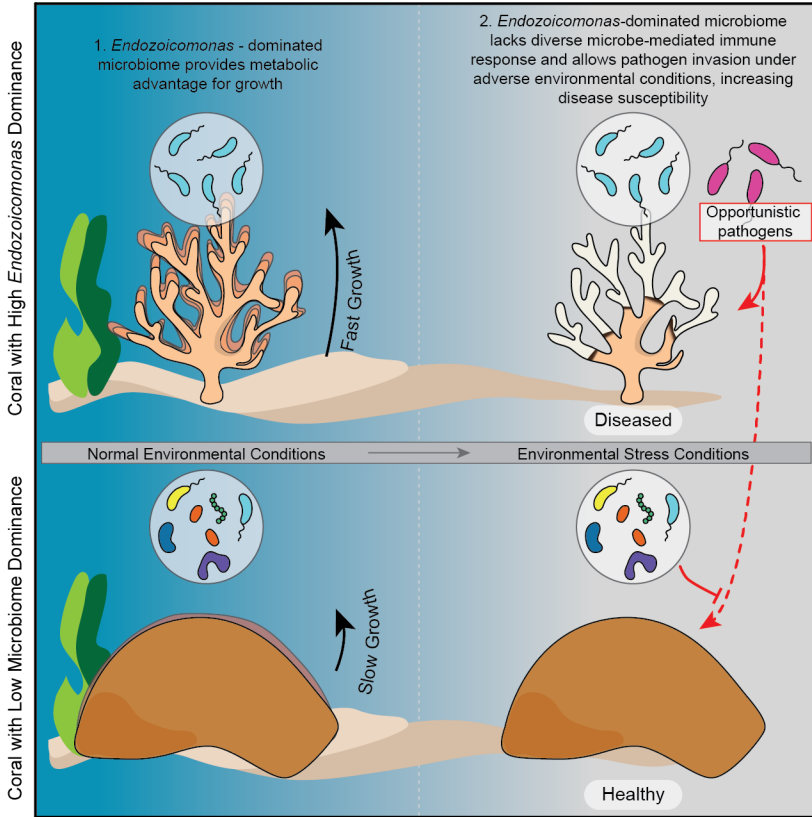
873 alpha and beta diversity metrics and disease, represented by the R² for PGLS correlations. Alpha
874 diversity metrics include richness, evenness (Gini index), and dominance (Simpson's index), and
875 weighted UniFrac beta diversity metrics including the three principal component axes (PC1, PC2,
876 PC3) that represent measures of community structure. Significant relationships ($p < 0.05$,
877 Supplementary Data Table 4) are marked by an asterisk (*). **C.** Bubble plot showing correlations
878 between dominant microbial taxa and coral disease prevalence. The size of each triangle
879 represents the R² for PGLS correlations between disease susceptibility and microbial relative
880 abundance for each listed taxon in either all samples (top row), mucus samples (cyan row), tissue
881 samples (orange row), or skeleton samples (purple row). Colored points were significant ($p <$
882 0.05, FDR q < 0.05) and hashed points were nominally significant ($p < 0.05$, FDR q > 0.05;
883 Supplementary Data Table 7a). Points that were not significant or had too little data ($n < 5$) for
884 reliable testing are marked in white. Taxa whose abundance is significantly correlated with
885 disease are marked in bold on the x-axis.

886



887

888 **Figure 3. *Endozoicomonas* correlates with growth and disease.** Phylogenetic independent
 889 contrasts in *Endozoicomonas* relative abundance in coral tissue (per 1000 reads) against **A.**
 890 microbial dominance, **B.** integrated estimate of coral disease prevalence and **C.** coral growth rate
 891 (mm per year) from the coral traits database. Dotted red lines in panels B and C indicate the null
 892 expectation that if traits are uncorrelated, change in the x-axis trait will not correlate with changes
 893 in the y-axis trait, with contrasts distributed equally above or below the dotted line. Statistics
 894 reflect phylogenetic generalized least squares (PGLS) regression (Supplemental Data Tables 5
 895 and 9). **D)** Modeled direction of causality between *Endozoicomonas* abundance, disease
 896 susceptibility and growth rate using both Brownian Motion (blue) and Pagel's Lambda (green,
 897 dotted) evolutionary models. The thickness of the lines represents the averaged standardized
 898 path coefficients of the top competing models based on CICc values (Supplementary Data Table
 899 12).



900
901
902
903
904

Figure 4. *Endozoicomonas* dominance facilitates life history tradeoffs. Conceptual hypothesis on the role *Endozoicomonas* (in teal) plays in the tradeoff between growth and defense (disease susceptibility) under varying environmental conditions.

Supporting Information for**Evidence for microbially-mediated tradeoffs between growth and defense throughout coral evolution**

Hannah E. Epstein¹, Tanya Brown², Ayomikun O. Akinrinade^{2,3}, Ryan McMinds^{1,4}, F. Joseph Pollock^{5,6}, Dylan Sonett⁷, Styles Smith⁵, David G. Bourne^{8,9}, Carolina S. Carpenter^{10,11}, Rob Knight¹¹⁻¹⁴, Bette L. Willis^{8,15}, Mónica Medina⁵, Joleah B. Lamb³, Rebecca Vega Thurber¹, Jesse R. Zaneveld^{2*}

¹Department of Microbiology, Oregon State University, 226 Nash Hall, Corvallis, OR 97331, USA

²School of Science, Technology, Engineering, and Mathematics, Division of Biological Sciences, University of Washington Bothell, UWBB-277, Bothell, WA 98011, USA

³Department of Ecology and Evolutionary Biology, University of California, Irvine, CA 92697, USA

⁴Center for Global Health and Infectious Diseases Research, University of South Florida, 13201 Bruce B. Downs Blvd, MDC 56, Tampa, FL 33612, USA

⁵Department of Biology, Pennsylvania State University, 208 Mueller Lab, University Park, PA 16802, USA

⁶Hawai'i & Palmyra Program, The Nature Conservancy, Honolulu, HI, USA

⁷School of Pharmacy, University of Washington, Seattle, WA 98195, USA

⁸College of Science and Engineering, James Cook University, Townsville, Queensland 4811, Australia

⁹Australian Institute of Marine Science, Townsville, Queensland 4810, Australia

¹⁰Scripps Institution of Oceanography, University of California, San Diego, La Jolla, CA 92093, USA

¹¹Center for Microbiome Innovation, University of California, San Diego, La Jolla, CA 92093, USA

¹²Department of Pediatrics, University of California, San Diego, La Jolla, CA 92093, USA

¹³Department of Computer Science & Engineering, University of California, San Diego, La Jolla, CA 92093, USA

¹⁴Micronoma Inc., San Diego, La Jolla, CA 92121, USA

¹⁵ARC Centre of Excellence for Coral Reef Studies, James Cook University, Townsville, Queensland 4811, Australia

*Jesse R. Zaneveld

Email: zaneveld@uw.edu

This PDF file includes:

Figures S1 to S4

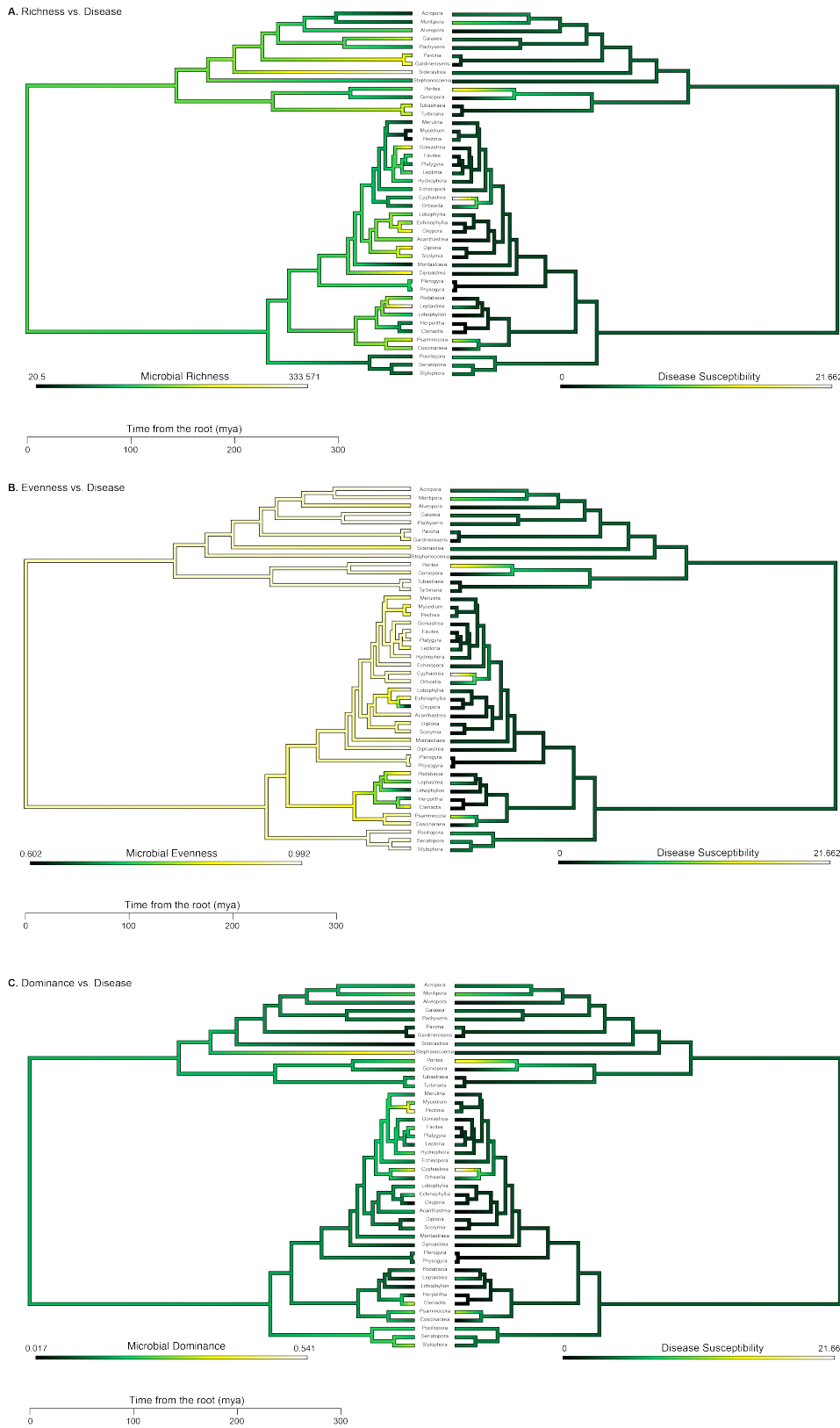


Fig. S1. Ancestral state reconstructions mirroring disease susceptibility and microbial alpha diversity metrics, including A) species richness, B) evenness (Gini Index), and C) dominance (Simpson's Index).

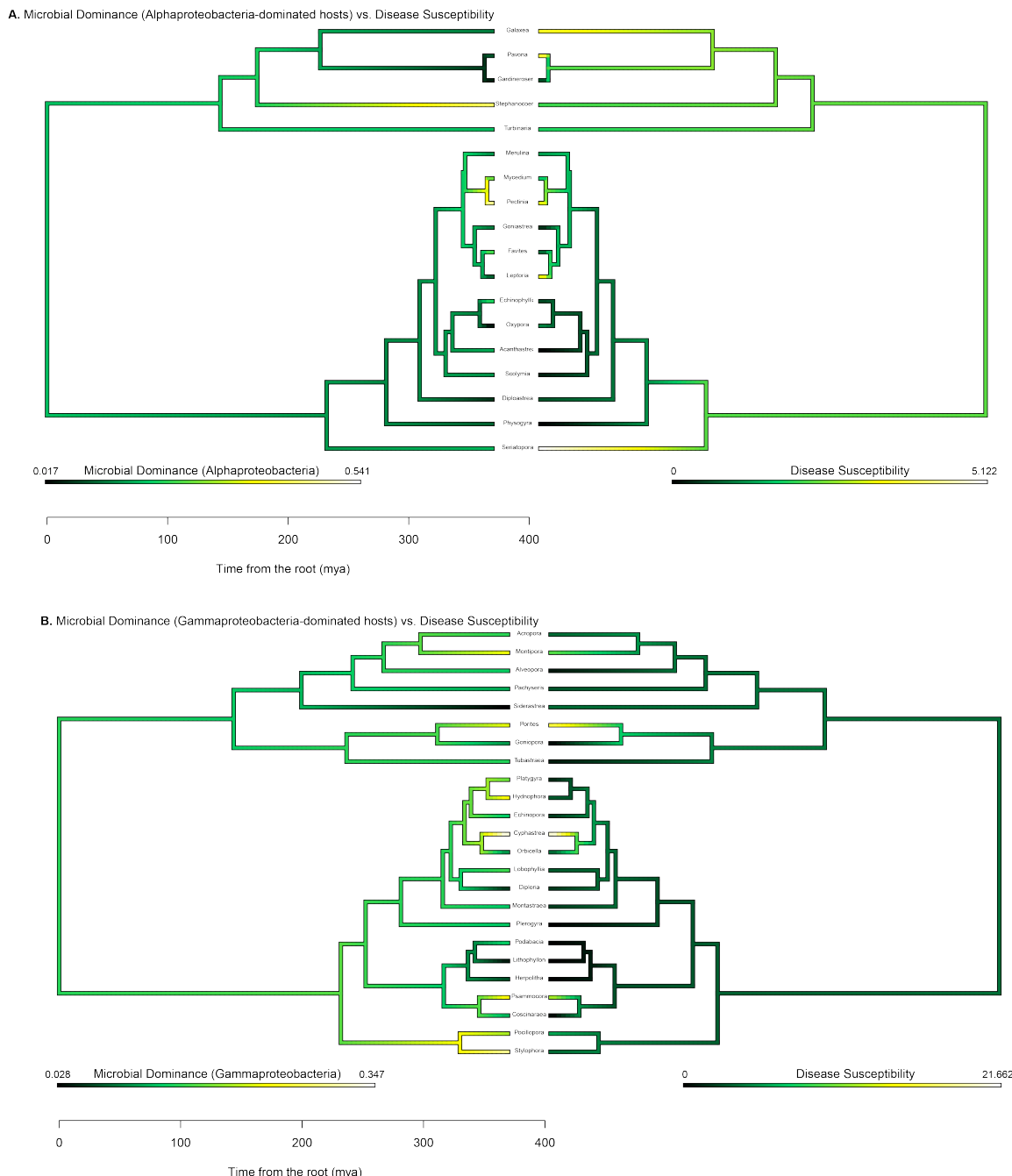


Fig. S2. Ancestral state reconstructions mirroring disease susceptibility and microbial dominance of A) Alphaproteobacteria only and B) Gammaproteobacteria only.

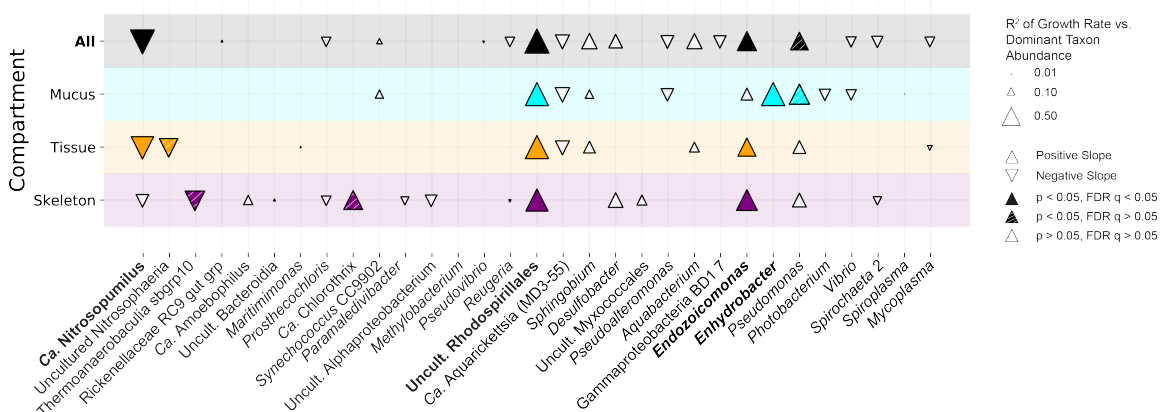


Fig. S3. Growth rate vs. dominant taxon abundance (zeros excluded). R^2 of the correlations between average coral host growth rate and dominant taxon relative abundance in corals only where each taxon is present (zero counts excluded). Arrow direction indicates a positive or negative correlation, filled arrows refer to significant correlations, striped arrows indicate nominally significant correlations (did not pass multiple comparisons) and open arrows indicate insignificant correlations. Size of the arrow represents R^2 value (See Supplementary Data Table 9b for details).

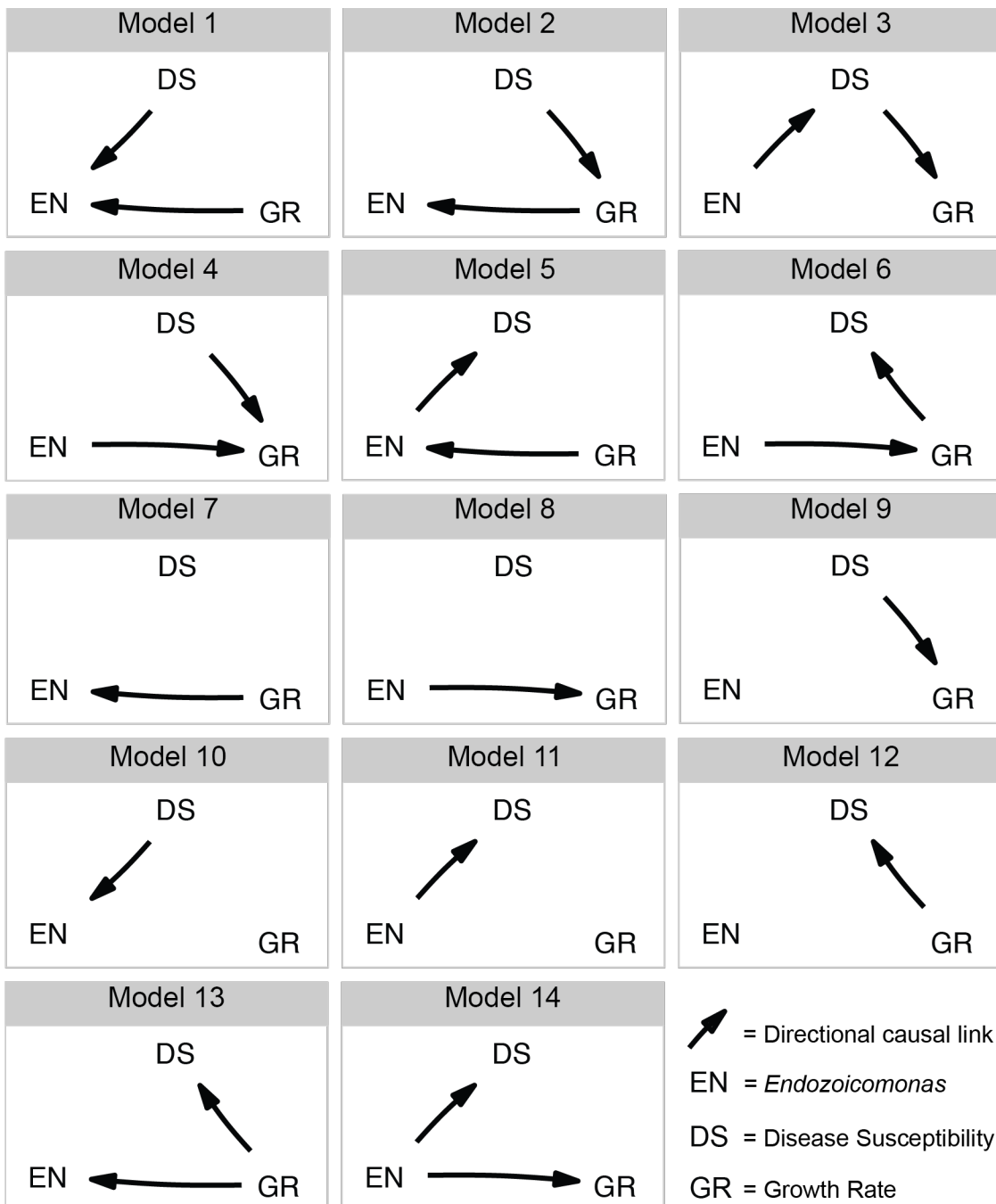


Fig. S4. Model selection for phylogenetic causality analysis. These models represent the fourteen plausible causality pathways that were used in the phylogenetic causality analysis. EN = *Endozoicomonas* relative abundance, DS = coral disease susceptibility, and GR = coral growth rate.